

# STRUCTURAL AND KINEMATICAL ANALYSIS OF MODEL OF SERIAL ROBOT

Ovidiu ANTONESCU, Politehnica University of Bucharest, oval33@hotmail.com

Mariana TROFIMESCU, High School Dinu Lipatti, Bucharest,  
banitamariana@yahoo.com

Paun ANTONESCU, Politehnica University of Bucharest, panton38@hotmail.com

**Abstract:** The paper presents a serial robot, whose main spatial kinematic chain consists of four revolute joints. Four continuous current electric motors are used for driving the serial robot. We carried out a structural analysis of the robot, which has four mobilities, while the fourth one is redundant. We have used matrix calculus for the kinematic analysis of the serial robot arm so that we obtained the three Cartesian coordinates of the characteristic points according to the four independent angular parameters. Regarding the prehension mechanism, the kinematic schema with two symmetrical parallelograms has been presented, which ensures the circular translational motion of the two fingers.

**Keywords:** kinematic schema, serial robot, mobility, matrix calculus, end effector.

## 1. The topological structure of robot arm

The robotic arm (fig. 1) is a serial type robot [5, 9, 10], including an open kinematic chain [1, 2] with spatial motion (fig. 1c).

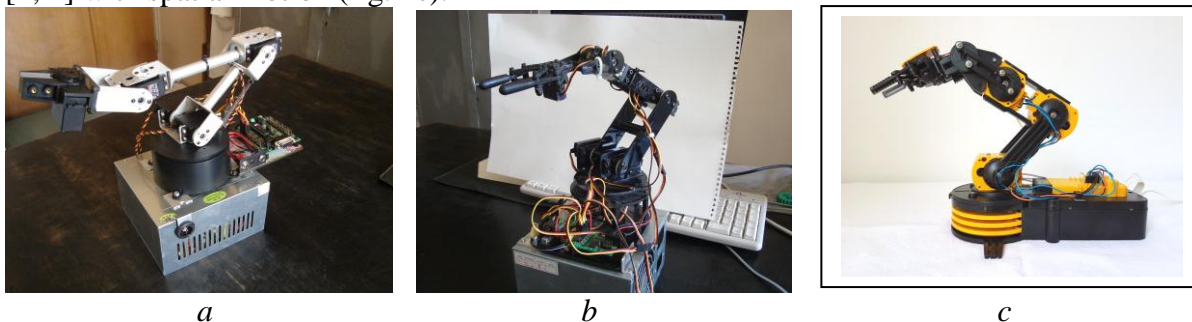


Fig. 1. Photos of the electrically driven serial robot [11]

The kinematic schema of the robotic arm (fig. 2) consists of a fixed standing point 0 around which the articulated kinematic chain moves in a horizontal plane.

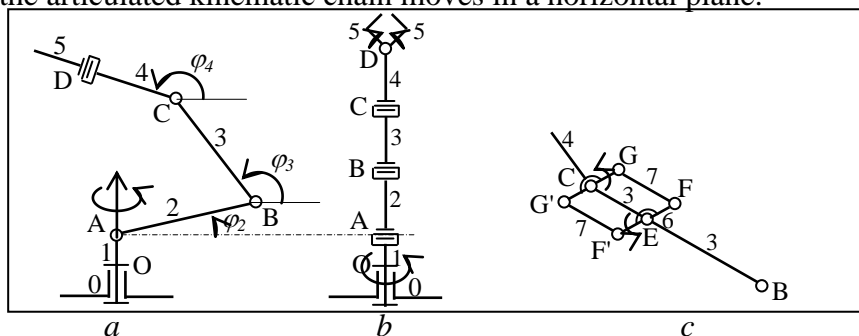


Fig. 2. Kinematic schema of the serial robot mechanism

The mobility of the open kinematic chain is given by the number of kinematic joints, which represent planar articulations (mono-mobile): O (with a vertical axis), A, B, C (with

parallel horizontal axes), and D (whose axis is perpendicular on the C axis). For the vertical position of the kinematic chain (fig. 2b), the articulation axis in D is horizontal.

By observing the kinematic schema (fig. 2), we identify five articulations, which means that the mobility of the serial robot is  $M_b = 5$ . The five main kinematic elements are driven by five continuous current electric motors, located right on or next to the axis of each articulation.

Each electric motor is geared with a worm-type reducer and spur gears. What is specific to this serial robot is the fact that the motor of the articulation in C is placed on bar 3 in point E (fig. 2c). From E, the motion is transmitted to the axis in C by means of two parallelogram dyadic chains (EFGC, EF'G'C) denoted as 6 and 7.

The articulation in D (fig. 2b) is double, consisting of two closed kinematic chains (4,5,8,9) of the parallelogram type (fig. 3).



Fig. 3. Photo (a) [11] and kinematic schema (b) of the prehension mechanism

Thus, a dyadic chain LD(8,9) is added to each bar 5, and the rotations of bars 5 (to the right and to the left) are obtained by means of a spur gear (fig. 3b).

The double articulation in D (fig. 2b) is in fact a plate 4 with four articulations D, D', D<sub>1</sub> and D'<sub>1</sub> (fig. 3b).

Each of the two gears is solidary with bar 5, the one to the left, respectively to the right (fig. 3). The two segments JK and J'K' are parallel, which allows for better prehension.

The mobility of the serial robot, equipped with two kinematic closed contours on bar 3 (fig. 2c), is then calculated using the formula [1, 3, 4]

$$M_b = \sum_{m=1}^5 m C_m - \sum_{r=2}^6 r N_r \quad (1)$$

The kinematic parameters of the mechanism (fig. 2) are in the matrix

$$\begin{bmatrix} C_1 & C_2 & C_3 & C_4 & C_5 \\ N_2 & N_3 & N_4 & N_5 & N_6 \end{bmatrix} = \begin{bmatrix} 11 & 0 & 0 & 0 & 0 \\ 0 & 2 & 0 & 0 & 0 \end{bmatrix} \quad (2)$$

Using formula (1) we deduce

$$M_b = 1 \times 11 - 3 \times 2 = 5 \quad (3)$$

Regarding the prehension mechanism that consists of articulated bars and gears (fig. 3), its mobility is calculated by means of formula (1), where structural parameters are given in the matrix

$$\begin{bmatrix} C_1 & C_2 & C_3 & C_4 & C_5 \\ N_2 & N_3 & N_4 & N_5 & N_6 \end{bmatrix} = \begin{bmatrix} 8 & 1 & 0 & 0 & 0 \\ 0 & 3 & 0 & 0 & 0 \end{bmatrix} \quad (4)$$

Substituting these parameters in formula (1) we deduce

$$M_b = (1 \times 8 + 2 \times 1) - 3 \times 3 = 1 \quad (5)$$

The mobility of the entire mechanism of the serial robot (fig. 2), including the prehension mechanism (fig. 3), is deduced by means of formula (1) and the matrix of specific parameters is

$$\begin{bmatrix} C_1 & C_2 & C_3 & C_4 & C_5 \\ N_2 & N_3 & N_4 & N_5 & N_6 \end{bmatrix} = \begin{bmatrix} 19 & 1 & 0 & 0 & 0 \\ 0 & 5 & 0 & 0 & 0 \end{bmatrix} \quad (6)$$

Substituting these numerical data, we obtain

$$M_b = (1 \times 18 + 2 \times 1) - 3 \times 5 = 5 \quad (7)$$

Besides the mobility of the prehension mechanism (fig. 3), the serial robot has four mobilities, which shows that the robot is hyper-redundant [7] since a point in 3D is defined by three Cartesian coordinates.

## 2. The geometry and kinematics of the robot arm type RRRR

Let us consider the spatial kinematic chain of the RRRR type, having the geometrical configuration  $R \perp R \parallel R \parallel R$  (fig. 4), which can be used as a positioning mechanism [6, 8] in the structure of a serial robot.

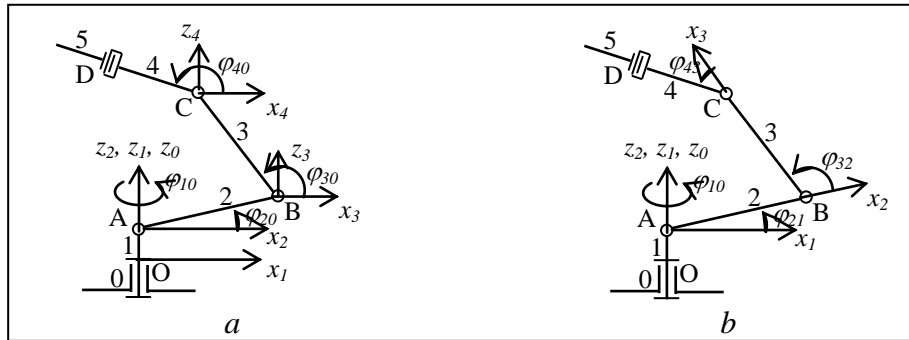


Fig. 4. Systems of coordinates used in direct kinematics

Let us choose the systems of Cartesian coordinates conveniently (fig. 4b): the fixed system  $Ox_0y_0z_0$  linked to the robot base; the mobile system  $Ax_1y_1z_1$  with the origin in the second articulation of element 1; the mobile system  $Bx_2y_2z_2$  whose origin is in the second articulation of element 2; the mobile system  $Cx_3y_3z_3$  whose origin is at the end of arm 3.

The constant parameters of the RRRR kinematic chain are (fig. 4):

$$OA = a_1; AB = d_2; BC = d_3; CD = d_4.$$

The variable parameters of the robotic arm are (fig. 4b):

$$\angle(x_0, x_1) = \varphi_{10} = \varphi_1; \angle(x_1, x_2) = \varphi_{21}; \angle(x_2, x_3) = \varphi_{32}; \angle(x_3, x_4) = \varphi_{43}$$

The direct kinematics of the serial robot type RRRR, with four rotational joints  $(\varphi_1, \varphi_2, \varphi_3, \varphi_4)$ , entangles calculating the position of the end point (characteristic)  $D$  using the Cartesian coordinates  $(x_D, y_D, z_D)$ , obtaining three functions dependent on the four independent geometrical parameters:

$$x_D = f_x(\varphi_1, \varphi_2, \varphi_3, \varphi_4); \quad y_D = f_y(\varphi_1, \varphi_2, \varphi_3, \varphi_4); \quad z_D = f_z(\varphi_1, \varphi_2, \varphi_3, \varphi_4).$$

$$\begin{bmatrix} x_D \\ y_D \\ z_D \end{bmatrix} = \begin{bmatrix} (d_2 \cos \varphi_{20} + d_3 \cos(\varphi_{20} + \varphi_{32}) + d_4 \cos(\varphi_{20} + \varphi_{32} + \varphi_{43})) \cos \varphi_{10} \\ (d_2 \cos \varphi_{20} + d_3 \cos(\varphi_{20} + \varphi_{32}) + d_4 \cos(\varphi_{20} + \varphi_{32} + \varphi_{43})) \sin \varphi_{10} \\ a_1 + d_2 \sin \varphi_{20} + d_3 \sin(\varphi_{20} + \varphi_{32}) + d_4 \sin(\varphi_{20} + \varphi_{32} + \varphi_{43}) \end{bmatrix} \quad (8)$$

The method of the square matrices  $4 \times 4$  (screw-matrix) uses the formula

$$\{\bar{r}_0\}_{4 \times 1} = [S_{01}]_{4 \times 4} \cdot [S_{12}]_{4 \times 4} \cdot [S_{23}]_{4 \times 4} \cdot [S_{34}]_{4 \times 4} \cdot \{\bar{r}_3\}_{4 \times 1} = [T_{04}]_{4 \times 4} \cdot \{\bar{r}_4\}_{4 \times 1}. \quad (9)$$

where:

$$\begin{aligned} [S_{01}]_{4 \times 4} &= \begin{bmatrix} \cos \varphi_1 & 0 & \sin \varphi_1 & 0 \\ \sin \varphi_1 & 0 & -\cos \varphi_1 & 0 \\ 0 & 1 & 0 & a_1 \\ 0 & 0 & 0 & 1 \end{bmatrix}; [S_{12}]_{4 \times 4} = \begin{bmatrix} \cos \varphi_2 & -\sin \varphi_2 & 0 & d_2 \cos \varphi_2 \\ \sin \varphi_2 & \cos \varphi_2 & 0 & d_2 \sin \varphi_2 \\ 0 & 0 & 1 & 0 \\ 0 & 0 & 0 & 1 \end{bmatrix}; \\ [S_{23}]_{4 \times 4} &= \begin{bmatrix} \cos \varphi_3 & -\sin \varphi_3 & 0 & d_3 \cos \varphi_3 \\ \sin \varphi_3 & \cos \varphi_3 & 0 & d_3 \sin \varphi_3 \\ 0 & 0 & 1 & 0 \\ 0 & 0 & 0 & 1 \end{bmatrix}; [S_{34}]_{4 \times 4} = \begin{bmatrix} \cos \varphi_4 & -\sin \varphi_4 & 0 & d_4 \cos \varphi_4 \\ \sin \varphi_4 & \cos \varphi_4 & 0 & d_4 \sin \varphi_4 \\ 0 & 0 & 1 & 0 \\ 0 & 0 & 0 & 1 \end{bmatrix}; \{\bar{r}_4\}_{4 \times 1} = \begin{bmatrix} 0 \\ 0 \\ 0 \\ 1 \end{bmatrix}. \end{aligned} \quad (10)$$

The transfer matrix  $[T_{04}]_{4 \times 4}$  is the product of the four screw-matrices in (10):

$$\begin{aligned} [T_{04}]_{4 \times 4} &= [S_{01}]_{4 \times 4} \cdot [S_{12}]_{4 \times 4} \cdot [S_{23}]_{4 \times 4} \cdot [S_{34}]_{4 \times 4} = \\ &= \begin{bmatrix} c\varphi_1 c(\varphi_2 + \varphi_3 + \varphi_4) & -c\varphi_1 s(\varphi_2 + \varphi_3 + \varphi_4) & s\varphi_1 & (d_2 c\varphi_2 + d_3 c(\varphi_2 + \varphi_3) + d_4 c(\varphi_2 + \varphi_3 + \varphi_4))c\varphi_1 \\ s\varphi_1 s(\varphi_2 + \varphi_3 + \varphi_4) & s\varphi_1 c(\varphi_2 + \varphi_3 + \varphi_4) & -c\varphi_1 & (d_2 s\varphi_2 + d_3 s(\varphi_2 + \varphi_3) + d_4 s(\varphi_2 + \varphi_3 + \varphi_4))c\varphi_1 \\ s(\varphi_2 + \varphi_3 + \varphi_4) & c(\varphi_2 + \varphi_3 + \varphi_4) & 0 & a_1 + d_2 s\varphi_2 + d_3 s(\varphi_2 + \varphi_3) + d_4 s(\varphi_2 + \varphi_3 + \varphi_4) \\ 0 & 0 & 0 & 1 \end{bmatrix} \end{aligned} \quad (11)$$

where we have used the notations for the final expression:

$$c = \cos, s = \sin, \varphi_2 = \varphi_{20}, \varphi_3 = \varphi_{32}, \varphi_4 = \varphi_{43}.$$

We notice the identity of the first three terms of the last column in (11) with the column matrix to the right of the matrix equation (8).

The Cartesian coordinates of point D are calculated by means of the formulas:

$$\begin{aligned} x_D &= (d_2 \cos \varphi_2 + d_3 \cos(\varphi_2 + \varphi_3) + d_4 \cos(\varphi_2 + \varphi_3 + \varphi_4)) \cos \varphi_1; \\ y_D &= (d_2 \cos \varphi_2 + d_3 \cos(\varphi_2 + \varphi_3) + d_4 \cos(\varphi_2 + \varphi_3 + \varphi_4)) \sin \varphi_1; \\ z_D &= a_1 + d_2 \sin \varphi_2 + d_3 \sin(\varphi_2 + \varphi_3) + d_4 \sin(\varphi_2 + \varphi_3 + \varphi_4). \end{aligned} \quad (12)$$

This proves relation (8) obtained from a square matrix  $3 \times 3$ .

### 3. Determining position functions for the RRRR robot

For the serial robot of the RRRR type (fig. 5), reversed kinematics results on the position functions:

$$\varphi_{10} = \varphi_1 = f_1(t); \varphi_{21} = \varphi_2 = f_2(t); \varphi_{32} = \varphi_3 = f_3(t); \varphi_{43} = \varphi_4 = f_4(t) \quad (13)$$

The Cartesian coordinates of the tracing point D are imposed in reversed kinematics, and the system of equations (12) deduced in direct kinematics is written as follows:

$$\begin{aligned}
(d_2 \cos \varphi_2 + d_3 \cos(\varphi_2 + \varphi_3) + d_4 \cos(\varphi_2 + \varphi_3 + \varphi_4)) \cos \varphi_1 &= x_D; \\
(d_2 \cos \varphi_2 + d_3 \cos(\varphi_2 + \varphi_3) + d_4 \cos(\varphi_2 + \varphi_3 + \varphi_4)) \sin \varphi_1 &= y_D; \\
d_2 \sin \varphi_2 + d_3 \sin(\varphi_2 + \varphi_3) + d_4 \sin(\varphi_2 + \varphi_3 + \varphi_4) &= z_D - a_1.
\end{aligned} \tag{14}$$

In general, for the robot we have considered (fig. 4), the system of equations (14) has a singular solution only for angle  $\varphi_1$ . Thus, we may deduce angle  $\varphi_1$  from the first two equations using the formula

$$\varphi_1 = \arctg\left(\frac{y_D}{x_D}\right) \tag{15}$$

If we select a certain value for angle  $\varphi_4$ , we eliminate angle  $\varphi_1$  from the first two equations (14), and we obtain the trigonometric equation

$$d_2 \cos \varphi_2 + d_3 \cos(\varphi_2 + \varphi_3) + d_4 \cos(\varphi_2 + \varphi_3 + \varphi_4) = \sqrt{x_D^2 + y_D^2} \tag{16}$$

Which together with the last equation of (14) forms the system of two non-linear equations:

$$\begin{cases} d_2 \cos \varphi_2 + d_3 \cos(\varphi_2 + \varphi_3) + d_4 \cos(\varphi_2 + \varphi_3 + \varphi_4) = \sqrt{x_D^2 + y_D^2}; \\ d_2 \sin \varphi_2 + d_3 \sin(\varphi_2 + \varphi_3) + d_4 \sin(\varphi_2 + \varphi_3 + \varphi_4) = z_D - a_1. \end{cases} \tag{17}$$

From system (17) we first determine angle  $\varphi_2$ , by eliminating angle  $(\varphi_2 + \varphi_3)$ , which leads to the trigonometric equation of the form:

$$A_2 \sin \varphi_2 + B_2 \cos \varphi_2 = C_2 \tag{18}$$

whose solution is given by the formula:

$$\varphi_2 = 2 \arctg\left(\frac{-A_2 \pm \sqrt{A_2^2 + B_2^2 - C_2^2}}{B_2 + C_2}\right) \tag{19}$$

In formula (19) we obtain two solutions for angle  $\varphi_2$  (fig. 5).

Angle  $\varphi_3$  is obtained in a similar manner, but it can also be determined directly from one of the two equations (17). The two solutions for angles  $\varphi_2$  and  $\varphi_3$  have been distinctly represented for the same position of the tracing point D respectively of the articulation C.

We shall consider the solution for which angle  $\varphi_2$  is smaller, which corresponds to the kinematic chain depicted by means of the continuous line (fig. 5).

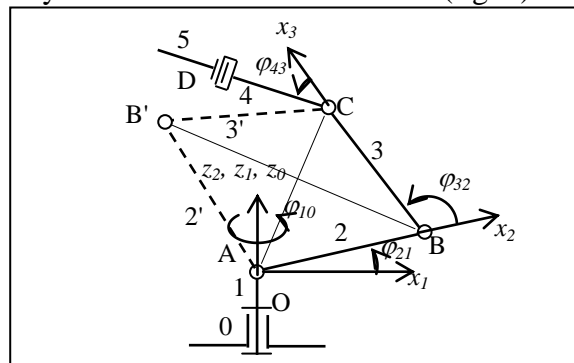


Fig. 5. The two solutions B and B' for the articulation (2,3)

The functional model of the serial redundant robot (fig. 1) allows the following limits of the rotation angles:  $\varphi_1 = 0^0, \dots, 270^0$  (fig. 6a),  $\varphi_2 = 0^0, \dots, 180^0$  (fig. 6b),  $\varphi_3 = 0^0, \dots, 300^0$  (fig. 6c) and  $\varphi_4 = 0^0, \dots, 120^0$  (fig. 6d).

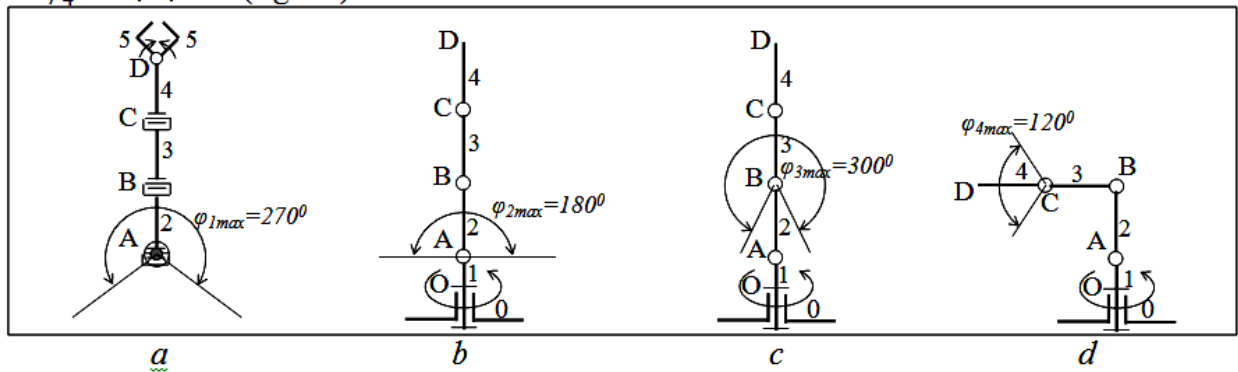
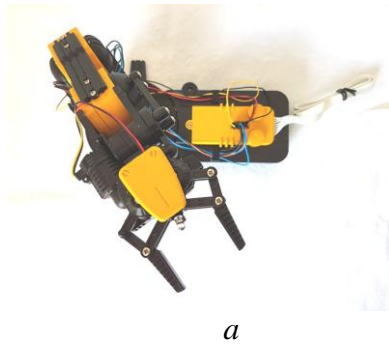


Fig. 6. Extreme rotations of the kinematic elements [11]

If we consider a median position of the kinematic chain plane, then angle  $\varphi_1$  will have the maximum value  $\varphi_{1max} = \pm 135^\circ$  (fig. 7a).



a



b

Fig. 7. Photos of the mechanical robotic arm [11]



c



d



e

Fig. 7. Photos of the mechanical robotic arm [11]

For angle  $\varphi_2$  we consider the vertical position of bar 2 as a median position (fig. 7c), so that angle  $\varphi_{2max} = \pm 90^\circ$ .

For bar 3, we also consider the vertical position as a median position (fig. 7d), which leads to the maximum value of angle  $\varphi_3 - \varphi_{3\max} = \pm 150^\circ$ . For bar 4, the median position is as a continuation of bar 3 (fig. 7b), and the maximum value of  $\varphi_4$  will be  $\varphi_{4\max} = \pm 60^\circ$ .

## References

- [1]. Antonescu, O., Antonescu, P., *Mechanism and Machine Science – course-book*, Politehnica Press, Bucharest, 2016;
- [2]. Antonescu, P., *General formula for the D.O.F. of complex structure manipulators and robots*, Proceedings of Tenth World Congress on the Theory of Machines and Mechanisms, Oulu, Finland, Vol. 2, pp. 1067-1072, 1999;
- [3]. Antonescu, P., Grecu, B., Rusu, M., *Analysis and synthesis of robot orientation mechanisms*, Construcția de mașini Journal, 54, No. 3, pp. 27-30, 2002;
- [4]. Antonescu, P., Antonescu, O., *Methods to determine the mobility (d.o.f.) of complex structure manipulators*, Mechanisms and Manipulators J., Vol. 3, No. 1, pp. 49-54, 2004;
- [5]. Staretu, I., *Structural synthesis and workspaces of the serial kinematic chains with 7 and 8 axes for industrial robots*, Robotics & Management J., Vol. 18, No. 2, pp. 21-25, 2013;
- [6]. Filip, V., Mateoiu, M.C., *Consideration on the use of manipulator-robots in the laser beam processing technology*, Mechanisms and Manipulators J., Vol. 2, No. 1, pp 51-56, 2003;
- [7]. Nitu, I., Cononovici, S. B., Racovita, W., *Using the redundancy of plane manipulators to avoid restriction areas*, Mechanisms and Manipulators J., Vol. 3, No. 2, pp. 65-72, 2002;
- [8]. Antonescu, P., *Mechanisms and Manipulators – applications – project topics*, Printech Publishing House, Bucharest, 2000;
- [9]. Doroftei, I., *The Architecture and Kinematics of Robots*, Cermi Publishing House, Iasi, 2002;
- [10]. Ramirez, D., Kotlarski, J., Ortmaier, T., *Automatic generation of serial manipulators to be used in a combined structural geometrical synthesis*, Mechanisms, transmissions and applications, Proceedings of the Third MeTrApp Conference, pp. 239 - 247, 2015;
- [11]. \*\*\* *Instructions - build your own mechanical robot arm*, Taiwan.